JCTC Journal of Chemical Theory and Computation

Microscopic Picture of the Aqueous Solvation of Glutamic Acid

Elske J. M. Leenders, Peter G. Bolhuis, and Evert Jan Meijer*

Van 't Hoff Institute for Molecular Sciences, Universiteit van Amsterdam, Nieuwe Achtergracht 166, 1018 WV Amsterdam, The Netherlands

Received December 19, 2007

Abstract: We present molecular dynamics simulations of glutamic acid and glutamate solvated in water, using both density functional theory (DFT) and the Gromos96 force field. We focus on the microscopic aspects of the solvation—particularly on the hydrogen bond structures and dynamics—and investigate the influence of the protonation state and of the simulation method. Radial distribution functions show that the hydrogen bonds are longer in the force field systems. We find that the partial charges of the solutes in the force field simulations are lower than the localized electron densities for the quantum simulations. This lower polarization decreases the hydrogen bond strength. Protonation of the carboxylate group renders glutamic acid a very strong and stable hydrogen bond donor. The donated hydrogen bond is shorter and lives longer than any of the other hydrogen bonds. The solute molecules simulated by the force field accept on average three more hydrogen bonds than their quantum counterparts. The life times of these bonds show the opposite result: the residence times are much longer (up to a factor 4) in the ab initio simulations.

1. Introduction

Glutamic acid, or its deprotonated equivalent glutamate, is one of the 20 natural amino acids. Solvated in water, it exists in zwitterionic form, see Figure 1. Next to being a building block in almost all proteins, glutamate also serves as a ligand in receptor proteins.[1] Our interest in this molecule arose as a result of our previous simulation research on the protonation reaction in the photocycle of the photoactive yellow protein (PYP).[2] This signaling protein has a chromophore[3,4] that responds to UV light and isomerizes from the cis to the trans state. We studied the solvation of this chromophore in detail.[5] After the isomerization, the chromophore is protonated, most likely by the nearby glutamic acid. When glutamic acid loses a proton, it takes up a negative charge. We showed that the reactive event involves the enhanced stabilization of glutamate by hydrogen bonds.[2] In the ground state of the protein, glutamic acid takes part in only one hydrogen bond: the one it donates to the negatively charged chromophore. When deprotonated, glutamate is only stable when it accepts at least three hydrogen bonds. This implies that upon proton transfer, hydrogen bonds in the environment of glutamate have to rearrange. They can be donated not only by surrounding amino acids or the chromophore but also by water molecules that penetrate the chromophore binding pocket of the protein.[6] We found that the hydrogen bond rearrangements occur easier and faster in force field molecular dynamics simulations of the protein, compared to QMMM (quantum mechanics/molecular mechanics) simulations that simulate glutamate and some of its possible hydrogen bond donors with quantum methods and the environment (protein and water molecules) with a force field.

These findings underline the importance of a proper description of the hydrogen bonding of glutamate and glutamic acid (both abbreviated as Glu) in the modeling of PYP. We therefore study the solvation of Glu in water, the prototype hydrogen bonding environment. Sun et al.[7] studied Glu in the gas phase with different quantum methods. Prabhakar[8] simulated a small part of the Glu side chain in a model system with three water molecules in the gas phase. Both systems are too small to see hydrogen bond exchanges. Experimental and quantum simulation studies on glutamic

* Corresponding author phone: +31-20-525-5265; fax: +31-20-525-5604; e-mail: ejmeijer@science.uva.nl.

10.1021/ct700344f CCC: $40.75
Published on Web 05/15/2008

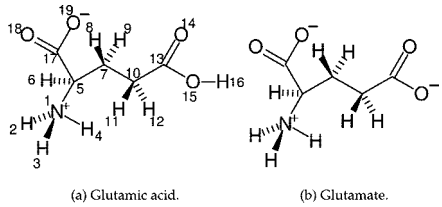

Figure 1. Glutamic acid (a) and glutamate (b). The two molecules differ in the protonation state of oxygen 15. At neutral pH, the amino acid is a zwitterion and the side chain is deprotonated, as its pK_a value is 4.07.

acid and glutamate solvated in water focus on spectroscopic properties.[1,9] Nowadays, classical simulations on simple systems as glutamic acid aim to optimize the parametrization of the force field.[10–14] They focus on the force field, not on glutamic acid itself, and they reproduce macroscopic thermodynamic quantities such as the density and the free enthalpies of solvation. To our knowledge, their is no previous work that investigates the microscopic and dynamic properties of glutamic acid and glutamate in solution.

We present in this paper a study on both protonation states of Glu in water, simulated with either a quantum or a force field method. Besides giving us a detailed picture of the hydrogen bonds and their dynamics in solution, this helps us to better interpret force field and QMMM results on PYP in previous and future work. The intention of this work is 1) to provide a microscopic picture of solvated Glu, focusing on aspects that have not or cannot be measured in experiments and 2) to understand what the influence of the simulation method is, so that we can interpret simulations of Glu correctly (not only in solvent but also in a protein environment).

In the next section, we explain how we equilibrated our systems and which simulation methods we used for our production runs. In the Results section, we compare various aspects of the simulations in different subsections and discuss them. In the concluding section, we summarize these results and show their impact on other simulations, such as our calculations on the photoactive yellow protein.

2. Computational Methods. As input structures, we equilibrated glutamic acid and glutamate in 135 SPC waters using the Gromos96 force field[15] (version G43a1) with the Gromacs software package.[16] The waters could form more than one solvation shell even when the molecule was extended. For all our force field simulations we used a time step of 2 fs and a Nosé-Hoover thermostat[17] with $\tau = 0.1$ ps, keeping the temperature at 300 K. The LINCS[18] and SETTLE[19] algorithms constrained the bond lengths and angles. For both systems we started with an NPT simulation of 2 ns, using the isotropic Berendsen barostat[20] with $\tau = 1$ ps and a reference pressure of 1 bar. Using the final configuration as a starting point, we performed NVT simulations of 2 ps with iteratively chosen box sizes. We took the box with the pressure nearest to 1 bar as a starting point for our production runs. For glutamic acid, the cubic box had a size of 16.3395 Å; for glutamate this was 16.2949 Å. Our force field production runs started from here, simulating NVT for 10 ns. We also performed one force field simulation of glutamate in a box of size 37.2350 Å containing 1638 water molecules to check for finite size effects.

Table 1. Four Systems Described in This Paper

system	method	protonation	charge	time step (fs)	simulation time (ps)
QMH	Quickstep	protonated (glutamic acid)	0	0.5	15.632
QM-	Quickstep	deprotonated (glutamate)	−1	0.5	15.593
FFH	force field	protonated (glutamic acid)	0	2	10000
FF-	force field	deprotonated (glutamate)	−1	2	10000

From the same starting structures, we performed quantum molecular dynamics simulations based on density functional theory (DFT) using Quickstep,[21] which is part of the CP2K program package.[22] It uses a Born−Oppenheimer molecular dynamics (BOMD) algorithm, meaning that it calculates the ground-state electron density every time step and from that the forces on the ions. It employs a hybrid Gaussian and plane waves (GPW) basis set,[23] which makes efficient and accurate density functional calculations of large systems (up to 1000 atoms) possible. We used Goedecker-Teter-Hutter (GTH) pseudopotentials[24,25] and the TZV2P basis set.[21] As it serves well for simulating liquid water,[26] we used the BLYP functional.[27,28] The density cutoff for the plane-wave basis set was 280 Ry and the time step 0.5 fs. A Nosé-Hoover chain thermostat[29] with a chain length of 3 and a time constant of 1000 fs fixed the temperature at 300 K. Every SCF step, the energy was converged up to 1.10^{-5} Hartree. Every time step, we recorded the positions, velocities, and Mulliken charges of all the atoms. We simulated for almost 18 ps; the first 2 ps were considered to be equilibration time and not included to calculate the properties. Izvekov et al.[30] showed that there is no velocity autocorrelation anymore after 1 ps in a quantum simulation of 64 water molecules. We checked the radial distribution functions and Mulliken charges in our simulations as well, and they are converged within 2 ps.

We studied glutamic acid and glutamate in water. For every protonation state of this molecule, one simulation was performed using the force field, another using the quantum mechanical method. In Table 1, we add symbols to these four systems, which we will use throughout this paper.

3. Results

In this section we will discuss the differences between various parameters calculated in the four different systems. First we will discuss the charges localized on the atoms. Then we will compare the hydrogen bond structures around the amino acid molecules and finally the dynamics of these bonds.

3.1. Charges. One of the main differences between force field and ab initio simulations is that the former uses fixed (partial) charges on atoms, while the latter calculates the electron density and hence the charge distribution every time step on the fly. In this section we check the difference between these fixed charges and the calculated ones, on the

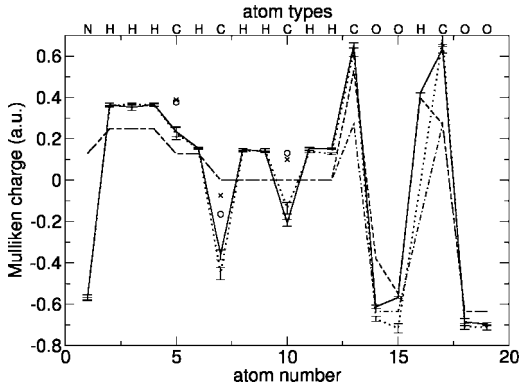

Figure 2. Mulliken charges on glutamic acid (system QMH, solid line) and glutamate (system QM-, dotted) and fixed force field charges for the systems FFH (dashed) and FF- (dashed-dotted). The numbers of the atoms agree with Figure 1. We also summed the Mulliken charges on the CH and CH_2 groups, to enable comparison with the force field, in which these hydrogens are implicit. For system QMH, the charge on these groups is represented by crosses, for system QM- by circles. The error bars give 1.96 times the standard deviation of the average of ten bins.

amino acid atoms and the water atoms. We distinguish between waters in the first solvation shell and bulk waters.

Figure 2 shows the average Mulliken charges on the atoms of the ab initio molecules, compared to the fixed charges of the force field. The force field does not include nonpolar hydrogens; the charge given is the charge of the complete CH or CH_2 group. Noticeable is that the two quantum simulations hardly differ in their partial charges. Only the charge on the two oxygens in the side chain carboxylate group differs, which can be expected as this is the group that is protonated in QMH and deprotonated in QM-. The differences however are very small. For most atoms, the force field charges are closer to zero than their quantum equivalents. This lower degree of polarization can lead to weaker hydrogen bonds in the force field simulations. Note that Mulliken charges are only one way to attribute charge densities to specific atoms; other methods might give somewhat different results. Although the force field partial charges are to some extent based on ab initio simulations, they have been adjusted to fit thermodynamic properties,[31] not to represent the charge density as good as possible. This being said, other researchers also saw the problem of the low polarization. Villa et al.[11] found too low values for the hydration free energies of many neutral amino acids with the Gromos96 force field. In that case, the results were in better agreement with experiments when all partial charges were multiplied with a factor 1.1.

Furthermore, while the N atom is very negatively charged in the DFT simulations (almost −0.6), it has a small positive charge of 0.13 in the force field. Although the hydrogen-bonding properties of the amino group are not the subject of this paper, this charge difference must influence these properties to some extent.

Table 2 shows the total charge on the Glu molecules. It shows that glutamic acid in system QMH has a small but significant positive charge. In the QM- case, the negative charge is not completely on the glutamate molecule but

Table 2. Total Charge on Glu in the Four Different Systems[a]

system	charge
QMH	0.0795 ± 0.0090
QM-	-0.643 ± 0.015
FFH	0
FF-	−1

[a] The error for the quantum systems is 1.96 times the standard deviation of the average of ten bins; the force field imposes an integer charge on the molecules.

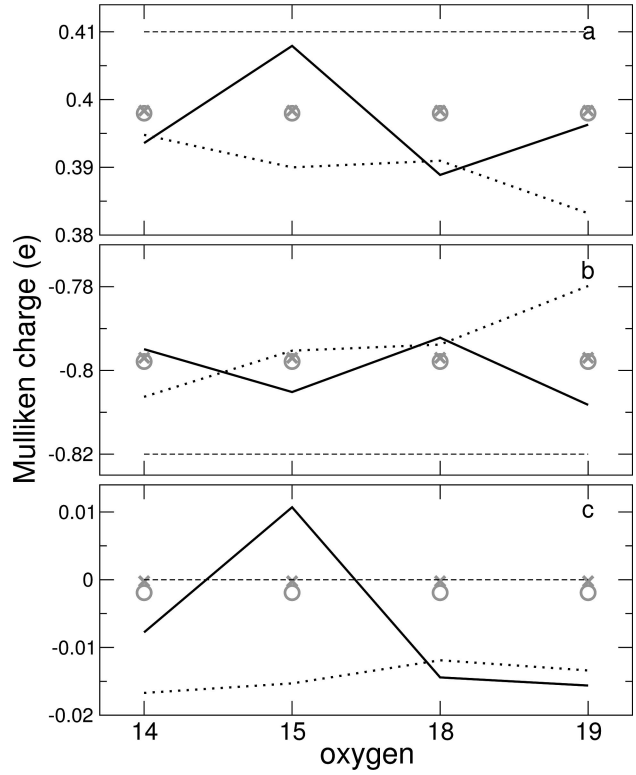

Figure 3. (Mulliken) charges on the water hydrogens (a) and the water oxygens (b) and the total charge per molecule (c). The dashed line is the constant charge from the force field simulations. The solid line represents the first solvation shell waters of QMH, the dotted line of QM-. The charges on bulk water molecules are given by the grey crosses (QMH) and circles (QM-). Note that the scales on the *y* axes differ. The indices on the *x* axis refer to the oxygen to which the waters hydrogen bond.

spread over the waters as well. Figure 3 is a visualization of the 'charge transfer' to the water molecules. It shows the (Mulliken) charges for the water molecules in the force field simulations and the quantum simulations, in the bulk and in the first solvation shell around the amino acid oxygens. Both the bulk and the first solvation shell waters of the QM-system are negatively charged, as could be expected from Table 2. The force field hydrogens in water are more positive than their quantum counterparts, the water oxygens more negative. Hence, force field water molecules are more polarized. This is in contrast with the solute molecules, that are more polar in the ab initio simulations.

Oxygen 15 is the protonated one in system QMH. The OH group influences the Mulliken charges of water molecules in its first solvation shell: only these molecules have

a positive charge, which is mainly caused by a larger positive charge on the water hydrogens (the oxygen is even more negative than in the bulk waters). This suggests that when glutamic acid donates a hydrogen bond, it transfers a part of the charge on the very positive hydrogen 16 to the accepting water molecule. This water molecule shows a higher polarization than bulk waters in the same simulation.

Another remarkable point is that oxygens in the same carboxylate group do not always show similar behavior. If we look at oxygen 18 and 19, the total charge of the water molecules in their solvation shell is almost the same, but the atomic charges vary. In QMH, we see that the water molecules around oxygen 18 are less polarized than bulk waters, but they are more polarized around oxygen 19. In QM-, it is exactly the other way around. This cannot be explained by the Mulliken charges on the oxygen atoms in Figure 2, as they are very similar. It is most likely an effect of different solvatation, perhaps because one of the groups is more sterically hindered than the other. Or, as the effect is opposite in the two different simulations, it can be accidental: a long-lasting hydrogen bond happens to point toward one of the oxygens, resulting in less space for possible hydrogen bond donors pointing toward the other. If this is the case, this is an unphysical effect caused by the short simulation times reachable with dynamical DFT simulations. Oxygens 14 and 15 also affect their first solvation shell in different ways in QM-, although less pronounced; we cannot compare this with the QMH simulation, as the protonation of oxygen 15 has a major influence. We will come back to this issue in section 3.2.2.

3.2. Structure. We compare the water structures around the Glu oxygens through the radial distribution functions of water oxygens and hydrogens. We also count the coordination numbers of water oxygens around the Glu oxygens, averaged over all frames. We saw no finite size effects in the structure calculations. The radial distribution functions from the small and large box are positioned exactly on top of one another; the maximum difference in the coordination numbers is 1%.

3.2.1. Radial Distribution Functions. In the FF- simulations, the structures around oxygens 14 and 15 are the same. The same holds for oxygens 18 and 19. For this reason, we present only the oxygen 14 and 18 results in Figure 4. The peaks in the radial distribution function for both carboxylate groups appear at the same distance but are more pronounced for the side chain oxygens. For the protonated case, oxygen 18 and 19 behave the same; their radial distribution functions are almost equal to the FF- results. However, the structures around oxygens 14 and 15 differ considerably (from each other and from the deprotonated results), see Figure 5. Both first hydrogen peaks are hardly present; the oxygen peaks are less pronounced than the oxygen peaks around oxygen 18 and 19 but still very clear. The oxygen−oxygen distance around oxygen 15 is much smaller than around oxygen 14. This indicates a very strong hydrogen bond between the protonated oxygen 15−acting as a hydrogen bond donor−and an accepting water molecule. It is likely that this strong bond disrupts the preferred water structure around oxygen 14, resulting in a less stable water network around this atom.

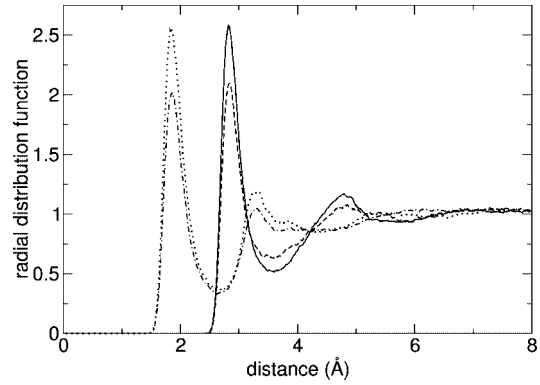

Figure 4. Radial distribution functions of water around Glu oxygens in system FF-. In both carboxylate groups, the two oxygens have the same distribution function. The solid line represents water oxygens around oxygen 14 (and 15), the dotted line water hydrogens around this oxygen. The dashed line shows water oxygens around oxygen 18 (and 19), the dashed-dotted lines the water hydrogens. All radial distribution functions in this paper are calculated over 1000 bins, presenting the results as running averages over 10 data points to smoothen the graphs.

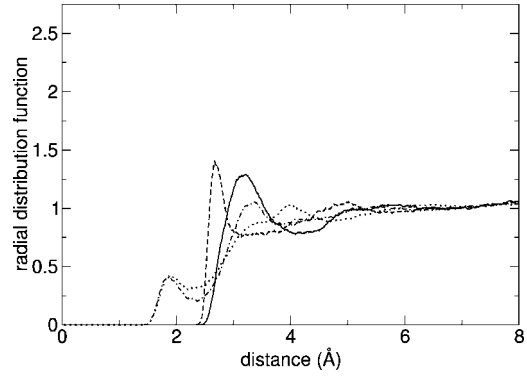

Figure 5. Radial distribution functions of water around the Glu oxygens in system FFH. The solid line represents water oxygens around oxygen 14, the dotted line water hydrogens around this oxygen. The dashed line shows water oxygens around oxygen 15, the dashed-dotted lines the water hydrogens. Around oxygen 18 and 19, the radial distribution function is exactly the same as for system FF- in Figure 4.

For the quantum simulations, we present the radial distribution functions in a different format: Figure 6 shows the water structure around oxygen 14 for both systems, Figure 7 around oxygen 15. For both graphs, the peaks are much more pronounced in system QM-. Around the nonprotonated oxygen 14, both simulations show their first peaks at the same distances. But for the QMH simulation, the first peaks are much lower and the second peaks are hardly visible, while they are clearly there for the QM- system. Apparently, the negative charge on the carboxylate group in system QM- stabilizes the water structure around it to a great extent. The graphs around oxygen 15 differ even more. The radial distribution functions around oxygen 14 and 15 are very similar in system QM-, although they are all slightly more prominent in the latter case. The first hydrogen peak around oxygen 15 is completely missing in system QMH (it is there in system FFH, though very small). This means that there are no water molecules that donate a hydrogen bond

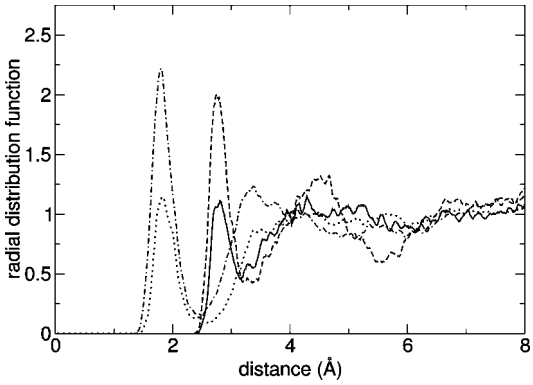

Figure 6. Radial distribution functions of water around oxygen 14 in both quantum simulations. The solid line shows the water oxygens and the dotted line the hydrogens around oxygen 14 in QMH. The dashed and dashed-dotted lines respectively show the same for QM-.

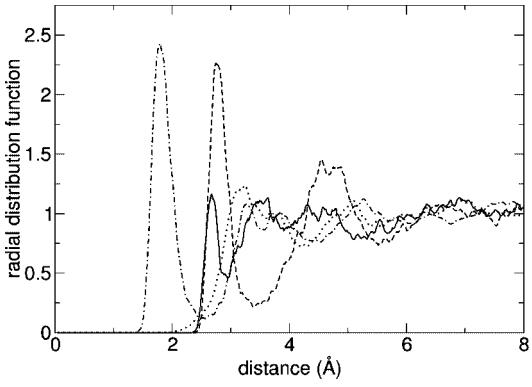

Figure 7. Radial distribution functions of water around oxygen 15 in both quantum simulations. The solid line shows the water oxygens and the dotted line the hydrogens around oxygen 15 in QMH. The dashed and dashed-dotted lines respectively show the same for QM-.

to it; the existence of a small oxygen peak shows that the glutamic acid OH group does take part in a hydrogen bond but as a donor. Because it can only donate one hydrogen bond, the surface below the peak is small. We will come back to this when we discuss the coordination numbers in section 3.2.2.

As the radial distribution functions around oxygen 18 and 19 in the quantum simulations are almost all the same, we present them in one figure, Figure 8. For the first peaks, both for water hydrogen and oxygen, the lines are very similar. Some dissimilarity occurs for the second solvation shell and further.

In the final radial distribution we present here, we compare the distribution of water around proton 16 in QMH and FFH (Figure 9). We see that the oxygen graphs show the same first peak, but the second peak is much clearer in the quantum simulation. The hydrogen peak is also sharper, but somewhat smaller, in this simulation compared to the force field system. The charge transfer of hydrogen 16 to water (see Figure 3) enhances the polarization of the water molecules in its solvation shell and hence strengthens the hydrogen bonds with the second solvation shell. Together with Figure 7, that lacks a peak for hydrogen around oxygen 15, we can conclude that the quantum oxygen 15 is chiefly a hydrogen

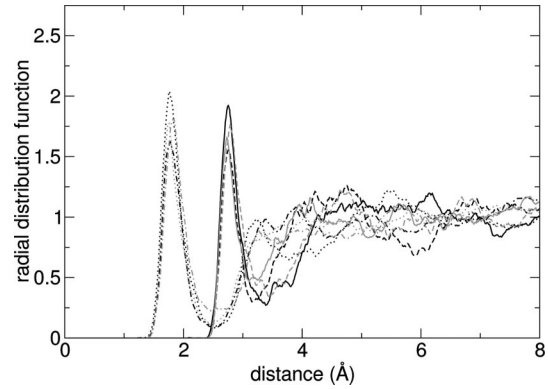

Figure 8. Radial distribution functions around oxygens 18 and 19 in the quantum simulations. The black lines refer to system QMH, the grey lines to system QM-. The solid lines show water oxygens and the dotted lines water hydrogens around oxygen 18. The dashed and dashed-dotted lines respectively show the same for oxygen 19.

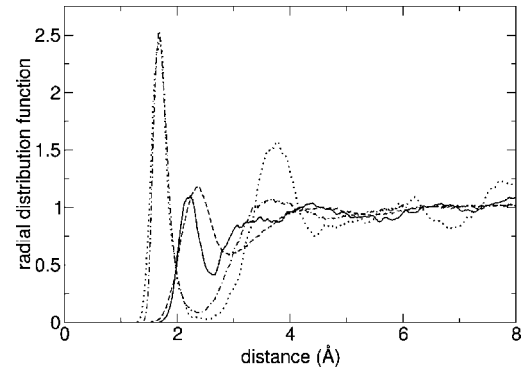

Figure 9. Radial distribution functions around hydrogen 16. The solid line shows the water hydrogen and the dotted line the water oxygen distribution in system QMH. The dashed and dashed-dotted lines respectively show the same in system FFH.

Table 3. Oxygen−Oxygen Distances for All Hydrogen Bonds, Taken from the Radial Distribution Functions[a]

atom	QM-	QMH	FF-	FFH
O_{14}	2.75 (3.22)	2.78 (3.17)	2.82 (3.59)	3.19 (4.09)
O_{15}	2.77 (3.39)	2.67 (2.95)	2.82 (3.59)	2.67 (3.14)
O_{18}	2.73 (3.11)	2.76 (3.39)	2.83 (3.56)	2.83 (3.51)
O_{19}	2.79 (3.44)	2.76 (3.17)	2.83 (3.56)	2.83 (3.51)
H_{16}		1.68 (2.48)		1.68 (2.37)

[a] All values are in Å. First we give the first maximum of the distribution function and after that between brackets the distance at the first minimum. Only in the case of proton 16, we give an oxygen−hydrogen distance (from the water oxygen to the Glu proton).

bond donor when protonated and hardly accepts any hydrogen bonds from water.

Table 3 gives an overview of the first peaks in all radial distribution functions. Overall, almost all hydrogen bond distances are slightly shorter in the quantum simulations. Also, the peaks are wider in the force field simulations. This is particularly the case for oxygen 14 in the protonated simulations. Only the donated hydrogen bond from oxygen 15 and proton 16 to water has the same length with both methods. This is in accordance with the lower polarization

shown in section3.1 for the force field, which results in weaker hydrogen bonds. This effect is corrected to a small extent by the somewhat higher polarization in the force field water molecules (see Figure 3). Note however that the *y* axis in Figure 2 has a much larger scale than in Figure 3: the polarization changes in the solute are a factor 3−10 times larger than in the solvent. It is likely that the newest parameter sets of the Gromos96 force field (53A5 and particularly 53A6) will show somewhat improved results for the hydrogen bond lengths. For these parameters, special attention is paid to fit hydration and solvation better, resulting in a remarkable improvements on the free enthalpies of solvation in water. For glutamic acid for example, this enthalpy is only 0.2 kJ/mol off the experimental value of −27.0 kJ/mol; version 43A2 gave a value of −16.2 kJ/mol.[10]

Unfortunately, we cannot compare these radial distribution numbers to experiments, as they have not been measured for water around Glu. What we can do−and we will make this comparison later in this paper as well−is look at what pure water simulations and experiments teach us. Pure water has been studied extensively with experiments, force field and quantum simulations; radial distribution functions are available for all three methods. The first peak is found at a distance of 2.73 Å with two different experimental methods.[32,33] With quantum methods this distance is between 2.69 Å and 2.78 Å,[33−36] for force field simulations between 2.69 Å and 2.86 Å.[33,34,37] The simulation methods closest to ours predict 2.75−2.78 Å for SPC water simulations[33,37] and 2.75 Å for a BOMD-BLYP simulation.[36] Most of the calculated values are close to the experimental ones; force field distances are on average somewhat more overestimated. Although the location of the peaks is predicted quite well, in many simulations the peaks are a bit too sharp and the first minima too deep. This overstructuring is more common in ab initio calculations than in force field tests. If we translate this result to our simulations−although we cannot be sure that solvation around Glu shows the same trends−we can conclude that the hydrogen bond distances are slightly better predicted by the QM simulations and the peak shape is better fitted by the force field.

3.2.2. Coordination Numbers. By calculating the coordination numbers, we know how many water molecules form a first solvation shell of a Glu oxygen. For every frame of our simulations, we count the number of water oxygens within the first solvation shell around each oxygen. For this purpose, we use a distance criterion taken from the radial distribution functions: the minimum after the first oxygen peak, with a maximum of 3.5 Å. To make sure that we count waters close to both oxygens of a carboxylate group only once, we assign it to the nearest Glu oxygen. Hence the coordination number for a certain oxygen is roughly the same parameter as the number of waters hydrogen bonding to it.

Figure 10 gives an overview of all average coordination numbers. Here we see that the total number of hydrogen bonds in the quantum simulations is always about 3 lower than in the corresponding force field simulation. The reason might be that the formation of hydrogen bonds in the force field is only induced by the (negative) charge on the oxygens. In the quantum simulation, the orbitals involved in the

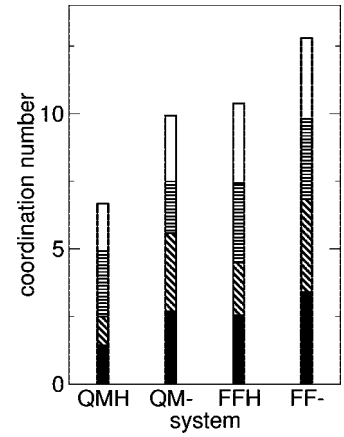

Figure 10. The coordination numbers for all systems and all Glu oxygens. The black bars give the average coordination number around oxygen 14, the diagonally striped bars around oxygen 15, the horizontally striped bars around oxygen 18, and the white bars around oxygen 19. The bars add up to give the total coordination number per amino acid.

hydrogen bonding have a distinct spatial distribution; hence, water cannot approach from any direction. Particularly, a carboxylate group has a resonance structure, with three lone pairs on one oxygen and two on the other. Because the force field cannot distinguish between the two, each oxygen can accept three hydrogen bonds. In a quantum simulation, the two states (one oxygen with a single bond to the carbon and one with a double bond) are distinguishable. On average, the electronic structure should be symmetric, but in a single time step it is not. We see this in our simulations when we look at the coordination and the C−O distance in each frame: the carboxylate oxygen with the lowest coordination number is usually the one with the shortest C−O distance and vice versa. This shows that the oxygen with the longer single bond to the carbon atom has more lone pairs. There is a similar pattern for the Mulliken charges on the oxygens: the oxygen with the higher coordination number has a more negative charge. The charge difference is small however, less than 0.1 e.

The average electronic structure is not perfectly symmetrical: the bars in Figure 10 do not have the same length for oxygens in the same carboxylate group, due to the fact that the exact electronic structure depends on the surrounding water structure as well. Our quantum simulations are not long enough for the water structure to switch numerous times between a coordination number of two and three around each oxygen.

The coordination around proton 16 is not shown in this picture (as it is included in the coordination around oxygen 15): it is 1.0 for both FFH and QMH, indicating that it is practically always donating the one hydrogen bond it can donate. However, the total coordination number of oxygen 15 equals 1 as well for QMH, while it is 2 in FFH. That means that oxygen 15 is an hydrogen bond acceptor as well in the force field simulation, but not in QMH. The protonation of oxygen 15 has more influence in QMH than in FFH, on the coordination of both oxygen 14 and oxygen 15.

The coordination numbers around oxygens 18 and 19 in the force field simulations are all very similar and close to 3. This was found as well by Speranskiy et al.,[1] who did stationary quantum simulations on solvated glutamate equilibrated by classical molecular dynamics, and by Alagona et al.,[38] who performed force field Monte Carlo on an acetate anion. In both these papers, the structure around the solute oxygens was calculated using a force field. The other carboxylate group, with oxygens 14 and 15, behaves in the same way in system FF-. However, for the quantum simulations the total coordination number per carboxylate groups is much less than 6. This is understandable, as the hydrogen bonds to the quantum oxygens are donated to five lone pairs at maximum. A coordination number of 4 per carboxylate group is already less common in the ab initio than in force field simulations. In order to reach high coordination numbers, the water molecules need to find a perfect position, adapting themselves not only to the Glu orbitals but also to the bulk water structure. When only the value of the charge matters, and not its spatiality—as is the case in the force field simulations—high coordination numbers are more common.

Villa et al.[11] found that the force field underestimates the free energy of hydration, as we discussed in section3.1. Our results show that this is not due to the number of hydrogen bonds: all force field simulations show an overcoordination. That means that it is most likely the strength of the bonds that is underestimated; this is in accordance with the longer hydrogen bonds in Table 3 and the lower polarization in Figure 2 for the force field solute. This effect is only compensated to a very small extent by the (much smaller) polarization increase of the force field water molecules shown in Figure 3.

Although the quantum simulations underestimate the coordination numbers compared to the force field, they overestimate the sharpness of the radial distribution peaks, as we showed in section3.2.1. We should actually identify two aspects of structure: 1) the distribution of hydrogen bond lengths (peak shape in the radial distribution function) and 2) the number of hydrogen bonds. Overstructuring of the first type is reported by ab initio studies on pure water, and our simulations show a similar behavior for water around Glu (see Table 3). In contrast, we find that for the second aspect the force field simulations overstructure compared to the ab initio calculations. This result is corroborated by the pure water results of Fernández et al.,[39] who also see a larger coordination number in force field compared to quantum simulations. We did not find any other pure water studies in literature that compare coordination numbers.

3.3. Dynamics. To compare the dynamical aspects of the hydrogen bond networks around glutamic acid and glutamate, we look at the residence times of the hydrogen bonds. Figure 11 shows the residence time of the water molecules around the oxygens of the chromophore. We defined a water molecule to be hydrogen bonded to a chromophore oxygen when the O−O distance was less than 3.5 Å and the O−H−O angle was more than 150°.[40] When a hydrogen bond deviated from this definition for less than 0.5 ps, the hydrogen bond was considered unbroken; when it existed for less than 0.5 ps, we did not take it into account when calculating the average residence time. In the quantum simulations, some residence times are of the same order of magnitude as the simulation times. Because we cannot say how much longer a water molecule would have donated or accepted a hydrogen bond after stopping the simulation, this implies that we can only provide a lower bound for the average hydrogen bond lifetime. The statistics of the force field residence times is much better, resulting in very similar values for oxygens in the same carboxylate group, as one would expect. In the quantum simulations, a single long residence time can influence the average significantly. Steric effects and the orbital structure play a role in the latter simulation too, so at least some part of the difference is physical.

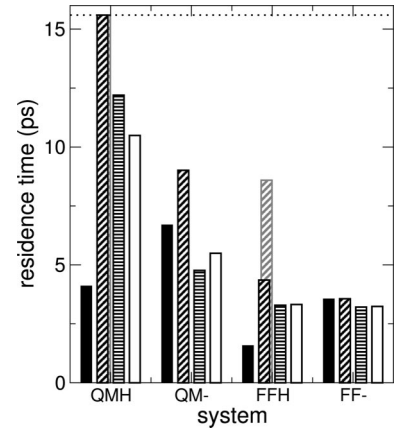

Figure 11. Residence times of water molecules hydrogen bonding to Glu oxygens. The horizontal dotted line indicates the total simulation time for the quantum simulations. The black bars correspond to oxygen 14, the diagonally striped bars to oxygen 15, the horizontally striped bars to oxygen 18, and the white bars to oxygen 19. When proton 16 was present, we represented the residence times of its donated hydrogen bond with the grey version of the oxygen 15 bar (as it is included in that residence time as well). In the QMH simulation, the residence times for oxygens 15 and proton 16 were exactly the same and therefore overlapping. In system FFH, the hydrogen bond donated by proton 16 lived about twice as long as the average hydrogen bond involving oxygen 15.

In spite of the fact that the quantum residence times might be somewhat underestimated, all of them are (much) longer than their force field counterparts. Especially in the protonated simulations, the difference is up to a factor 4. The tallest bar in Figure 11 is the result of one water molecule accepting a hydrogen bond from oxygen 15 and proton 16 during the complete QMH simulation. The special character of the hydrogen bond donated by oxygen 15 is exemplified by the fact that it is accepted by the only water molecule in the Glu solvation shell with a net positive charge (see Figure 3). The residence time could even be much longer than this, if we could simulate for longer times. Note however that the statistics here are poor: the 'average' residence time is calculated on the basis of only one hydrogen bond. The difference between the oxygen 15 residence times of system QM- and FF- is smaller but still large. In simulations of glutamate embedded in the photoactive yellow protein, we

saw too that the residence times of hydrogen bonds donated to Glu were shorter in force field simulations than in QMMM simulations.[2]

When force field water molecules move from one hydrogen bond acceptor to the other (for example from one carboxylate oxygen to the other or from glutamate to water), they move their positively charged hydrogen from one region of negative charge to the other. As the charge has no directionality, the proton will be somewhat stabilized by both acceptors when it is exactly in the middle of the transition. A quantum water in a quantum environment feels less electron density during the transition, as the orbital structure of the two acceptors only stabilizes the proton's positive charge when it is pointing in the right direction. This will make the barrier for hydrogen bond switching higher and the residence times longer.

Both the force field and the quantum simulations show the same trend on protonation: the residence time on oxygen 15 increases, while the hydrogen bonds donated to oxygen 14 have a shorter lifetime. Particularly in QMH we see that oxygen 15 is a very stable hydrogen bond donor when protonated. In FFH too, the hydrogen bonds donated by oxygen 15 last longer than the ones accepted by it. We saw this phenomena as well in our simulations of p-coumaric acid in water:[5] when the solute has an OH bond, which is more flexible than a C═O bond, it can more easily adapt to the water structure around it, and, hence, donated hydrogen bonds tend to be more stable than accepted ones on the oxygen in question. This flexibility effect compensates for the diminished stability due to fact that glutamic acid is now neutral and oxygens 14 and 15 are not as negative as in glutamate. For oxygen 14, only the latter destabilizing effect is present and hence it stabilizes its hydrogen bonds somewhat less.

When checking for finite size effects, we found that the life times of all the hydrogen bonds in simulation FF- are a factor 1.3 too long compared to the force field simulation in the large box. We do not expect that the size of the larger simulation box still has a substantial effect, because the box contains more than 6 solvation shells around Glu in each direction. Although we could not test the finite size effect for the quantum simulations, we expect that these effects are the same for the first principles simulations. In case of QMMM simulations of a full protein in water, this overestimation should be negligible, as the box sizes are many times larger than the ones in this work. So although we can still compare the life times of the hydrogen bonds presented here, they will most likely deviate from the 'real' values.

In studies of pure water, we did not find measurements of 'individual' hydrogen bond life times. We can look however at the calculated self-diffusion constants. Comparison of ab initio simulations of pure water with experiments and force field simulations[30,34–36,39,41–46] has shown that self-diffusion is difficult to calculate (separate simulations give results that differ up to 2 orders of magnitude) and often underestimated, especially when simulated ab initio. Some papers[34,35] state that this diminished mobility is due to an overcoordination of water (sharper peaks in the radial distribution function). We think it is not proven that this is the only or even the most important factor. The box sizes in these simulations were only 32−64 water molecules, sometimes not even comprising two full solvation shells in a cubic box. We have shown that the box size is an important factor, especially for dynamical properties.

4. Conclusions

When simulating the solvatation of glutamic acid and glutamate in water, it does matter which method one uses: based on a force field (Gromos96) or on DFT. With DFT-BLYP we see a larger variation in the strength and number of hydrogen bonds. This should be attributed to the fact that in the DFT method the electronic distribution in the molecules can adapt to the changing environment giving rise to changes in polarization, whereas in the force field method the partial charges on the atoms are fixed. This is not only of importance for the Glu atoms but also for the water molecules, particularly the ones in the first solvation shell.

Force field simulations tend to overcoordinate water molecules with about three extra hydrogen bonds per Glu molecule compared to quantum systems. Particularly the negatively charged carboxylate groups in the force field systems are very strong acceptors, accepting three hydrogen bonds per oxygen on average. In the quantum description the resonance structure of the carboxylate group has only five lone pairs, which are not always occupied by hydrogen bonds, as steric hindrance by the bulk water or glutamate itself does not allow it. This substantially decreases the average coordination number.

In the case of glutamic acid, the differences are most pronounced. The protonation decreases the coordination number around oxygen 15 drastically to 1 in system QMH, while it is almost 2 in FFH. The difference is similar on oxygen 14:1.5 vs 2.5. In the quantum simulation, we see a transfer of positive charge from proton 16 to the nearest water molecule. The hydrogens of this water become more positive and the oxygen more negative. This stronger polarization increases the lifetime of the bond significantly, up to values longer than the simulation time, that is at least 15.6 ps. In system FFH, the residence time of the average water molecule around oxygen 15 is only 4.4 ps. The accepting water molecule stays longer but only 8.6 ps on average. All the other residence times are much shorter in the force field than in the quantum simulations too.

The structural differences between the two methods are mainly that more waters hydrogen bond in force field simulations. The hydrogen bonds itself are not that much different; they are slightly longer in the force field description but within a range of 4%. Only one hydrogen bond differed more than that, almost 15%. The largest dissimilarity however is in the residence times. These times are always underestimated by the force field, sometimes up to a factor 4. Our results suggest that for a proper force field description of the aqueous solvation of glutamic acid and glutamate, the force field should allow for a varying and asymmetric charge distribution of the carboxylate group. This would accommodate an asymmetric coordination of the water molecules around the Glu oxygens as seen in our DFT-based simula-

tions. A stronger polarization (that is, a larger absolute value of the partial charges) will result in shorter and stronger bonds.

Fernández et al.[39] show a correlation between the self-diffusion coefficient of water and the number of defects. This effect is present in 'real' and simulated water, and it is not an unphysical result of the simulation method. The overcoordination in Glu in our force field simulations will induce more defects in the water structure than the ab initio simulation does, and this will make the water molecules more mobile. Although the diffusion is coupled to the lifetime of hydrogen bonds, it is not a one-to-one relation. Hydrogen bond switching is a more local phenomenon than self-diffusion, and estimates of hydrogen bond life times are likely to be better than diffusivity predictions. To properly estimate self-diffusion, a molecule should travel a significant distance, but in ab initio simulation times water molecules can barely move 1 Å. Summarizing, we should be well aware that we cannot draw strong conclusions on which simulation compares better to real Glu solvated in water: the force field or the ab initio simulation. Our errors are most likely less severe than in most of the pure water simulations that can be related to experiments, because of our larger box sizes and the focus on local processes. With ab initio simulations, one includes electron density spatiality, yielding a detailed picture of related properties such as coordination numbers and hydrogen bond switching events. But the time scale for changes in these properties is of the same order as the simulation times for quantum simulations, resulting in better sampling in the force field simulations. From the simulations presented in this paper we can understand, and to some extent quantify, the difference between force field and quantum simulations, in order to recognize unphysical effects around the border of QM and MM parts in combined simulations.

In relation to the simulation of the proton transfer in the photoactive yellow protein, it is interesting to know that the residence time changes upon protonation are much larger for the quantum system than for the force field system. The changes are also larger than the residence time differences upon protonation of the phenolic oxygen of p-coumaric acid in our previous paper.[5] This means that deprotonation of glutamic acid has a larger residence time decreasing effect than the opposite effect on the chromophore and, hence, that it is likely that the hydrogen bond between the two molecules in the protein breaks easier after the proton transfer. This indicates that a direct proton transfer from Glu to p-coumaric acid can be a starting point for the breaking of hydrogen bonds and ultimately unfolding of the protein. We also saw that upon deprotonation of Glu, glutamate attracts three extra hydrogen bonds to the now negatively charged carboxylate group−independent of the simulation method. In force field simulations of glutamate in the protein as well,[2] the number of hydrogen bonds increased from 1 to 4 in less than 10 ps. The need to stabilize the negative charge on Glu makes hydrogen bond rearrangements easier. Exactly these rearrangements are part of the process of unfolding the protein into its signaling state.

Acknowledgment. This work was sponsored by the Stichting Nationale Computerfaciliteiten (National Computing Facilities Foundation, NCF) for the use of the supercomputer facilities. We would like to thank the Nederlandse Organisatie voor Wetenschappelijk Onderzoek (Netherlands Organization for Scientific Research, NWO) for funding.

References

(1) Speranskiy, K.; Kurnikova, M. *J. Chem. Phys.* **2004**, *121*, 1516–1524.

(2) Leenders, E. J. M.; Guidoni, L.; Röthlisberger, U.; Vreede, J.; Bolhuis, P. G.; Meijer, E. J. *J. Phys. Chem. B* **2007**, *111*, 3765–3773.

(3) Hoff, W. D.; Düx, P.; Hård, K.; Devreese, B.; Nugteren-Roodzant, I. M.; Crielaard, W.; Boelens, R.; Kaptein, R.; Van Beeumen, J.; Hellingwerf, K. J. *Biochemistry* **1994**, *33*, 13959–13962.

(4) Baca, M.; Borgstahl, G. E. O.; Boissinot, M.; Burke, P. M.; Williams, D. R.; Slater, K. E.; Getzoff, E. D. *Biochemistry* **1994**, *34*, 14369–14377.

(5) Leenders, E. J. M.; VandeVondele, J.; Bolhuis, P. G.; Meijer, E. J. *J. Phys. Chem. B* **2007**, *111*, 13591–13599.

(6) Kamiya, M.; Saito, S.; Ohmine, I. *J. Phys. Chem. B* **2007**, *111*, 2948–2956.

(7) Sun, W.; Kinsel, G. R.; Marynick, D. S. *J. Phys. Chem. A* **1999**, *103*, 4113–4117.

(8) Prabhakar, R.; Blomberg, M. R. A.; Siegbahn, P. E. M. *Theor. Chem. Acc.* **2000**, *104*, 461–470.

(9) Jayaraman, V.; Keesey, R.; Madden, D. R. *Biochemistry* **2000**, *39*, 8693–8697.

(10) Oostenbrink, C.; Villa, A.; Mark, A. E.; Van Gunsteren, W. F. *J. Comput. Chem.* **2004**, *25*, 1656–1676.

(11) Villa, A.; Mark, A. E. *J. Comput. Chem.* **2002**, *23*, 548–553.

(12) Kaminski, G. A.; Friesner, R. A.; Tirado-Rives, J.; Jorgensen, W. L. *J. Phys. Chem. B* **2001**, *105*, 6474–6487.

(13) Cornell, W. D.; Cieplak, P.; Bayly, C. I.; Gould, I. R.; Merz, K. M.; Ferguson, D. M.; Spellmeyer, D. C.; Fox, T.; Caldwell, J. W.; Kollman, P. A. *J. Am. Chem. Soc.* **1995**, *117*, 5179–5197.

(14) Smith, B. J. *J. Comput. Chem.* **1999**, *20*, 428–442.

(15) Scott, W. R. P.; Hünenberger, P. H.; Tironi, I. G.; Mark, A. E.; Billeter, S. R.; Fennen, J.; Torda, A. E.; Huber, T.; Krüger, P.; Van Gunsteren, W. F. *J. Phys. Chem. A* **1999**, *103*, 3596–3607.

(16) Van der Spoel, D.; Lindahl, E.; Hess, B.; Van Buuren, A. R.; Apol, E.; Meulenhoff, P. J.; Tieleman, D. P.; Sijbers, A. L. T. M.; Feenstra, K. A.; Van Drunen, R.; Berendsen, H. J. C. Gromacs user manual, version 3.3; 2005. Gromacs Web site http://www.gromacs.org (accessed Dec 7, 2007).

(17) Hoover, W. G. *Phys. Rev. A* **1985**, *31*, 1695–1697.

(18) Hess, B.; Bekker, H.; Berendsen, H. J. C.; Fraaije, J. G. E. M. *J. Comput. Chem.* **1997**, *18*, 1463–1472.

(19) Miyamoto, S.; Kollman, P. A. *J. Comput. Chem.* **1992**, *13*, 952–962.

(20) Berendsen, H. J. C.; Postma, J. P. M.; Van Gunsteren, W. F.; DiNola, A.; Haak, J. R. *J. Chem. Phys.* **1984**, *81*, 3684–3690.

(21) VandeVondele, J.; Krack, M.; Mohamed, F.; Parrinello, M.; Chassaing, T.; Hutter, J. *Comput. Phys. Commun.* **2005**, *167*, 103–128.

(22) CP2K developers home page. http://cp2k.berlios.de (accessed Dec 7, 2007).

(23) Lippert, G.; Hutter, J.; Parrinello, M. *Mol. Phys.* **1997**, *92*, 477–487.

(24) Goedecker, S.; Teter, M.; Hutter, J. *Phys. Rev. B* **1996**, *54*, 1703–1710.

(25) Hartwigsen, C.; Goedecker, S.; Hutter, J. *Phys. Rev. B* **1998**, *58*, 3641–3662.

(26) Sprik, M.; Hutter, J.; Parrinello, M. *J. Chem. Phys.* **1996**, *105*, 1142–1152.

(27) Becke, A. D. *Phys. Rev. A* **1988**, *38*, 3098–3100.

(28) Lee, C.; Yang, W.; Parr, R. G. *Phys. Rev. B* **1988**, *37*, 785–789.

(29) Martyna, G. J.; Klein, M. L.; Tuckerman, M. *J. Chem. Phys.* **1992**, *97*, 2635–2643.

(30) Izvekov, S.; Voth, G. *J. Chem. Phys.* **2002**, *116*, 10372–10376.

(31) Hermans, J.; Berendsen, H. J. C.; Van Gunsteren, W. F.; Postma, J. P. M. *Biopolymers* **1984**, *23*, 1513–1518.

(32) Soper, A. K.; Bruni, F.; Ricci, M. A. *J. Chem. Phys.* **1997**, *106*, 247–254.

(33) Sorenson, J. M.; Hura, G.; Glaeser, R. M.; Head-Gordon, T. *J. Chem. Phys.* **2000**, *113*, 9149–9161.

(34) Schwegler, E.; Grossman, J. C.; Gygi, F.; Galli, G. *J. Chem. Phys.* **2004**, *121*, 5400–5409.

(35) Grossman, J. C; Schwegler, E.; Draeger, E. W.; Gygi, F.; Galli, G *J. Chem. Phys.* **2004**, *120*, 300–311.

(36) Kuo, I. W.; Mundy, C. J.; McGrath, M. J.; Siepmann, J. I. *J. Chem. Theory Comput.* **2006**, *2*, 1274–1281.

(37) Glattli, A.; Daura, X.; Van Gunsteren, W. F. *J. Chem. Phys.* **2002**, *116*, 9811–9828.

(38) Alagona, G. *J. Am. Chem. Soc.* **1986**, *108*, 185–191.

(39) Fernández-Serra, M. V.; Artacho, E. *J. Chem. Phys.* **2004**, *121*, 11136–11144.

(40) Luzar, A.; Chandler, D. *Phys. Rev. Lett.* **1996**, *76*, 928–931.

(41) Mills, R. *J. Phys. Chem.* **1973**, *77*, 685–688.

(42) Watanabe, K.; Klein, M. L. *Chem. Phys.* **1989**, *131*, 157167..

(43) Mahoney, M. W.; Jorgensen, W. L. *J. Chem. Phys.* **2001**, *114*, 363–366.

(44) Kuo, I. W.; Mundy, C. J.; McGrath, M. J.; Siepmann, J. I.; VandeVondele, J.; Sprik, M.; Hutter, J.; Chen, B.; Klein, M. L.; Mohamed, F.; Krack, M.; Parrinello, M. *J. Phys. Chem. B* **2004**, *108*, 12990–12998.

(45) Asthagiri, D.; Pratt, L. R.; Kress, J. D. *Phys. Rev. E* **2003**, *68*, 041505.

(46) Silvestrelli, P. L.; Parrinello, M. *J. Chem. Phys.* **1999**, *111*, 3572–3580.

CT700344F